Proceedings of 5th International Conference CNDGS'2026

ISSN 2669-2023 (print) / ISSN 2538-8959 (on-line) / **https://doi.org/ 10.47459/cndcgs.2026.19**

Stand-Off Distance Influence on Jet Performance of 3D-Printed Shaped Charge Liners

Michal Bilina[1], Martin Vítek[2], István Ember[3], Ota Rolenec[1]

[1]Department of Engineer Support, Faculty of Military Leadership, University of Defence, Address: Kounicova 65, 662 10, Brno, Czech Republic
[2]Department of Weapons and Ammunition, Faculty of Military Technology, University of Defence, Address: Kounicova 65, 662 10, Brno, Czech Republic
[3]Combat Support Department, Faculty of Military Sciences and Officer Training, Ludovika University of Public Service, Address: Ludovika tér 2, 1083, Budapest, Hungary

*Correspondence:**michal.bilina@unob.cz

Abstract

This paper evaluates the influence of extended stand-off distance on the performance of 3D-printed copper-filled shaped charge liners. The study follows a previous experiment in which complete perforation was achieved at stand-off distances of 0, 15, 30 and 60 mm. Two additional distances, 100 and 150 mm, were tested using the same charge configuration. The results were assessed qualitatively based on penetration morphology. Complete perforation was achieved in all cases, but the 150 mm configuration showed reduced channel regularity and probable loss of jet coherence. The most favorable morphology was observed at 60 mm.

KEY WORDS: *3D printing; shaped charge; CopperFill; stand-off distance; material extrusion; EOD; penetration morphology*

Citation: Bilina, M.; Vítek, M.; Ember, I.; Rolenec, O. Stand-Off Distance Influence on Jet Performance of 3D-Printed Shaped Charge Liners. In Proceedings of the Challenges to National Defence in Contemporary Geopolitical Situation, Brno, Czech Republic, 7-10 September 2026. ISSN 2538-8959, https://doi.org/ 10.47459/cndcgs.2026.19

1. Introduction

One of the dynamically developing areas in the modernization of armed forces is the systematic integration of additive manufacturing into training and logistical processes [1]. Within the Army of the Czech Republic, increased attention has been devoted in recent years to the implementation of polymer-based 3D printers in unit preparation, particularly in the fields of training and technical support. At present, 3D printers are available at several units, and their utilization is gradually expanding. [2]

A significant application area is the production of training aids, especially mock-ups of both foreign and domestic ammunition. These models represent a cost-effective solution, as their acquisition costs are low and, in the event of damage or loss, they can be quickly and inexpensively reproduced in the required quantities. This approach enables a flexible response to current training requirements without imposing a substantial financial burden [3]. With the increasing availability of 3D printing technology, new possibilities have also emerged in the field of combat engineering support [4]. Additive manufacturing has been used for some time in the production of shaped charge liners, employing filaments with various material additives [5]. These materials have a significant influence on the resulting mechanical and ballistic properties of the printed components, creating opportunities for systematic experimental research and optimization of their functional parameters [6].

One of the promising directions for further development is the use of improvised or field-fabricated special charges capable of destroying ammunition or cutting and separating its structural components within the scope of EOD and C-IED tasks. Such applications place high demands on the safety, reliability, and effectiveness of the employed means [7]. To ensure the required level of safety and functionality, it is therefore essential to conduct targeted research in the field of 3D printing

of shaped charge liners as well as complete charges utilizing standardized explosives, particularly plastic explosives. A key aspect is understanding the behaviour of shaped charge liners manufactured using polymer additive technologies, including the influence of the applied materials on their mechanical and ballistic properties. Knowledge of these characteristics is crucial for assessing the real operational applicability of additively manufactured components and for further optimization of their structural design.

2. Background and Previous Experiment

The previous study [5] focused on the experimental evaluation of shaped charges manufactured with the support of material extrusion 3D printing. The aim was to compare the effect of charges without a liner and charges equipped with a 3D printed copper-filled shaped charge liner. The experiment was conducted at the "Hanácká louka" blasting pit in the Březina military area in the Czech Republic.

The charge bodies, stand-off distance supports and packers were produced using a Prusa MK4 3D desktop printer. Each charge was filled with 250 g of Semtex 90 PH plastic explosive. In the first configuration, shown in Figure 1(a), the shaped cavity was formed directly in the explosive using a packer. In the second configuration, shown in Figure 1(b), a 3D-printed liner manufactured from ColorFabb CopperFill filament was inserted into the pre-formed cavity.

The CopperFill filament consisted of a PLA-based polymer matrix filled with copper powder, allowing the liner to be manufactured using a standard material extrusion process. However, this material should not be regarded as interchangeable with conventional PLA filament. Due to the high proportion of copper filler, CopperFill exhibits substantially different density, printability, abrasive behaviour, thermal response, and mechanical properties compared to unfilled PLA.

The tested stand-off distances of 0, 15, 30 and 60 mm are shown schematically in Figure 1(c). These distances were created using 3D-printed support pads placed between the charge and the steel target. A steel cylinder with a diameter of 250 mm, a length of 500 mm, and a wall thickness of 32 mm was used as the target. The material was identified as unalloyed E355 steel containing approximately 1.5% molybdenum and 0.5% silicon. Hardness was measured according to ISO 6506 using a Zwick ZHU 2.5 hardness tester and reached 178 ± 8 HBW 5/25.

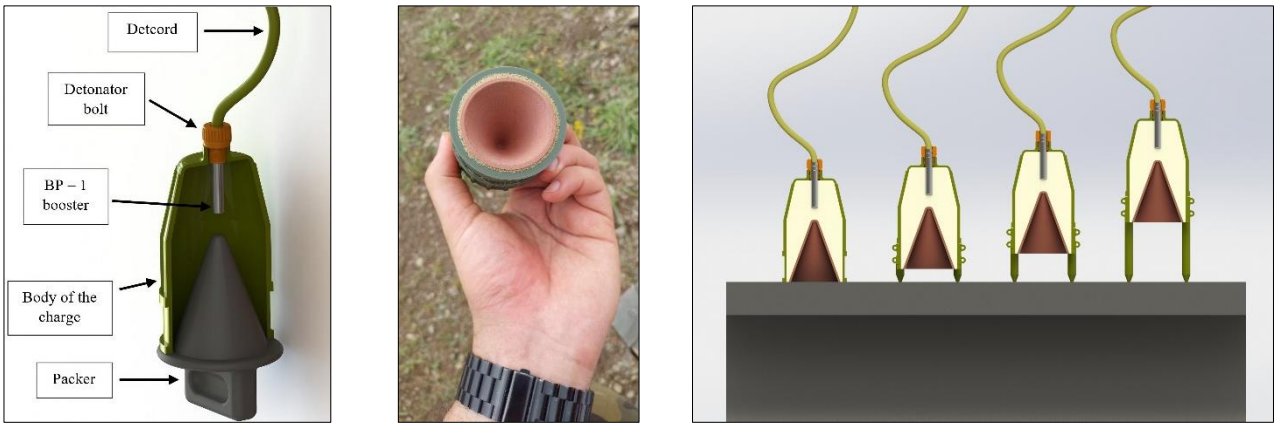

(a) (b) (c)

Figure 1. Experimental configuration of the 3D-printed shaped charge: (a) charge assembly with the main components, (b) 3D-printed copper-filled liner inserted into the charge body, and (c) schematic representation of the tested stand-off distances in the previous experiment.

The previous study confirmed that shaped charges equipped with 3D-printed copper-filled liners were capable of penetrating the steel target at all tested stand-off distances. In all cases, complete penetration was achieved, and the resulting holes showed typical features of a concentrated shaped charge effect, including relatively narrow openings, sharp edges and visible copper residues on the internal surfaces.

However, this result also limited the interpretation of the previous experiment. Since all lined charges penetrated the target, the tested range of 0–60 mm was insufficient to identify a clear trend in the influence of stand-off distance on penetration performance and hole geometry. The previous study therefore confirmed the functionality and effectiveness of 3D-printed copper-filled liners, but did not determine the distance at which their performance starts to decrease. The present follow-up experiment addresses this limitation by extending the tested stand-off distances to 100 and 150 mm.

2.1 Results of previous experiment

The following subsection summarizes the key results of the previous experiment that are relevant for the present follow-up study. Only the charges equipped with 3D-printed copper-filled liners are considered, because the objective of the present paper

is to extend the evaluation of stand-off distance for this liner configuration. The results are summarized in Figure 2 and further illustrated by the sectioned samples shown in Figure 3.

(a) (b) (c)

Figure 2. Overall result of the previous experiment with 3D-printed copper-filled liners: (a) arrangement of the shaped charges with 3D-printed liners on the steel target before detonation; (b) steel target after detonation, showing the four rear entrance holes corresponding to the lined charge configuration; (c) outlet holes on the inner side of the steel cylinder corresponding to the tested stand-off distances.

The previous experiment showed that the addition of a 3D-printed copper-filled liner substantially changed the penetration morphology produced in the steel target. As shown in Figure 2, all four charges equipped with liners achieved complete perforation of the cylinder wall. The entrance holes were clearly visible on the outer surface of the cylinder, while the outlet holes on the inner side confirmed that the jet effect was sufficient to pass through the full wall thickness.

The sectioned samples in Figure 3 provide a more detailed view of the penetration morphology at the originally tested stand-off distances of 0, 15, 30 and 60 mm. Although complete penetration was achieved in all cases, the morphology of the holes was not identical. The 0 mm configuration produced a relatively wide and strongly deformed channel, indicating intensive local interaction between the liner and the target surface at very short distance. At 15 and 30 mm, the channels remained continuous, but visible deformation and irregularities were still present. The 60 mm configuration produced the most regular penetration among the previously tested distances, with a narrower channel and limited deformation of the surrounding material.

These observations suggested that the effect of stand-off distance was already visible within the original experiment, but the tested range was not sufficient to identify the point at which the penetration effect begins to degrade. Since all lined charges perforated the steel wall, the previous study confirmed the functionality of the 3D-printed liner but could not determine the upper effective stand-off range. This was the main motivation for extending the experiment to 100 and 150 mm in the present study.

(a) (b)

(c) (d)

Figure 3. Sectioned samples from the previous experiment showing the effect of stand-off distance on penetration geometry for charges equipped with 3D-printed copper-filled liners: (a) 0 mm; (b) 15 mm; (c) 30 mm; (d) 60 mm.

3. Methodology

The methodology of the follow-up experiment was based on the same experimental configuration as in the previous study. The charge design, target material, liner concept, initiation method and evaluation procedure were kept unchanged in order to ensure comparability of the results. The only intentional modification was the extension of the tested stand-off distance range.
While the previous experiment evaluated stand-off distances of 0, 15, 30 and 60 mm, the present follow-up experiment added two larger values, namely 100 and 150 mm. These distances were selected to determine whether the performance of the 3D-printed copper-filled liner remains effective beyond the previously tested range, or whether a decrease in penetration performance and hole quality becomes observable at larger stand-off distances.
The use of an unchanged experimental setup was essential for the interpretation of the results. Since the charge configuration and target material remained the same, the observed differences can be attributed primarily to the change in stand-off distance rather than to changes in charge geometry, liner design, explosive mass or target properties.
The perforated samples produced by the action of a shaped-charge jet were first separated from the remaining part of the tube using a mechanical saw. The separated specimens were subsequently sectioned in the vertical plane of perforation using a cooled metallographic cutting saw in order to expose the internal geometry of the penetration channel. The cut surface was then mechanically ground using P60 abrasive paper. To enhance the contrast of the observed surface and reduce excessive image brightness, the ground surface was etched with a 2% Nital solution. Nital is a metallographic etchant consisting of nitric acid dissolved in alcohol and is commonly used for etching metallic materials and revealing the microstructure, particularly in steels and ferrous alloys [8]. After surface preparation, the specimens were documented using an Olympus DSX1000 opto-digital microscope at a magnification of 24×.

3.1 Experimental design

The experiment was conducted at the same test site as the previous study, namely the Hanácká Louka blasting area in Březina, Czech Republic. Two charges with identical charge bodies, liners, explosive mass and initiation arrangement were used, differing only in the applied stand-off distance, as shown in Figure 4(b). The preparation procedure for the individual charges is illustrated in Figure 4(a).
Each charge was filled with 250 g of Semtex 90 PH plastic explosive, which is commercially supplied in 500 g packages. After filling, the charges were weighed to verify that their explosive masses were consistent. The steel target was secured to prevent displacement during the test.
Both charges were detonated within a single firing event using a parallel detonation cord initiation network. The two branches of the detcord network were prepared with equal lengths of detonation cord in order to ensure, as far as practicable, simultaneous initiation of both charges.

(a) (b)

Figure 4. Experimental setup of the follow-up stand-off distance test: (a) preparation and mass verification of the charge components; (b) placement of the charges on the secured steel target prior to initiation.

3.2 Charge configuration

The charges were designed and manufactured using the same procedure as in the previous experiment. With the exception of the detonator screw, all components were manufactured by material extrusion using a Prusa MK4 3D printer equipped with an enclosure. The detonator well was designed to correspond to the structural configuration used in selected types of charges introduced in the Czech Armed Forces. This arrangement made it possible to secure the detonation cord primer using a detonator screw.
Conventional PLA filament was used to manufacture the charge body and the support structures required to establish the stand-off distance. The shaped charge liners, shown in Figure 5(a), were manufactured from CopperFill filament produced by

ColorFabb. According to the manufacturer, this filament has a density of approximately 4 g/cm³ and consists of approximately 80% copper powder and 20% PLA [9]. The PLA matrix allows the material to be processed using standard material extrusion technology. However, due to the high content of metallic filler, the use of a hardened nozzle with a diameter of 0.6 mm was required.

The liner geometry was selected to correspond to the conventional shape of liners used in standard ammunition. The liner was printed with 100% infill. Due to the liner wall thickness of 2 mm, the wall was formed by four perimeters, i.e., continuous contour paths deposited by the nozzle across successive layers. Using perimeter-only printing was also intended to improve geometrical homogeneity around the vertical axis, which is important for the symmetry and function of a shaped charge liner. The internal cone angle of the liner was 40°. The liner height was 60 mm, and its maximum diameter at the wider end was 50 mm. The final liner mass was 37 g.

The support structure used to establish the stand-off distance consisted of two parts enclosing the lower section of the charge body, as shown in Figures 5(b) and 5(c). After being attached to the charge, both halves of the support structure were fastened together using binding wire. In the 150 mm stand-off distance configuration, the support structures were additionally reinforced with cross braces to increase their stiffness and maintain the required geometry during preparation and placement of the charge.

(a) (b) (c)

Figure 5. Design of the 3D-printed liner and stand-off support structures used in the follow-up experiment: (a) geometry of the 3D-printed copper-filled liner; (b) charge configuration with the support structure for 100 mm stand-off distance; (c) charge configuration with the reinforced support structure for 150 mm stand-off distance.

3.3 Visual evaluation criteria

Due to the experimental character of the test and the limited availability of precise dimensional measurements, the evaluation was primarily qualitative. The assessment was based on photographic documentation of the target after detonation and on visual inspection of the sectioned samples. The main objective was not to establish exact numerical penetration parameters, but to compare the resulting penetration morphology with the previously tested stand-off distances.

The evaluation was structured according to the visual criteria listed in Table 1. Particular attention was paid to the appearance of the entrance and exit holes, including their shape, regularity, burr formation and visible deformation. The internal morphology of the penetration channel was assessed in terms of channel wall roughness, tearing, visible copper-covered areas and tapering from the entrance side towards the exit side. The apparent alignment of the jet was evaluated based on visible deviation or asymmetry of the penetration channel. Finally, the quality of the exit-side edge was assessed according to the presence of sharpness, tearing, melting-like effects or irregular deformation around the hole. These criteria were used to compare the newly tested stand-off distances with the previous results obtained for 0, 15, 30 and 60 mm.

Table 1. Qualitative visual criteria for the evaluation of penetration morphology

Criterion	What is assessed
Entrance hole	Shape, regularity and visible deformation around the impact-side opening
Exit hole	Shape, regularity, burrs and deformation on the outlet side
Channel wall morphology	Roughness, tearing and visible copper-covered areas inside the penetration path
Channel tapering	Visual change in channel width from entrance to exit
Jet alignment	Obvious deviation or asymmetry of the penetration channel
Exit-side edge quality	Sharpness, tearing, melting-like effects or irregular deformation around the hole

4. Results

The results section presents the penetration morphology produced by the newly tested stand-off distances of 100 and 150 mm and compares these results with the previously evaluated configurations of 0, 15, 30 and 60 mm. Since all lined charges achieved complete perforation of the steel wall, the evaluation focuses primarily on qualitative differences in the entrance and exit holes, penetration channel morphology, channel tapering, jet alignment and edge quality.

4.1 Result at 100 mm stand-off distance

Figures 6(a) and 6(b) show the left and right sections of the penetration channel produced in the steel cylinder segment by the charge equipped with a 3D-printed copper-filled liner at a stand-off distance of 100 mm. Figure 6(c) shows the corresponding front view of the entrance hole. The section indicates that the shaped-charge jet was slightly deviated from the charge axis. This is also reflected in the asymmetric deformation around the entrance hole, where local material build-up is visible on only one side of the opening. The entrance hole is relatively wide, and its surrounding area shows more pronounced plastic deformation of the target surface. This deformation suggests intensive interaction between the jet and the steel cylinder surface during the initial phase of penetration.

Nevertheless, the penetration channel remains continuous and relatively regular along its full length. Although the cut edges around the channel are locally deformed, no pronounced burr formation, extensive material tearing, or severe disruption of the channel walls is visible. The internal surface of the hole is rough, but without major irregularities that would indicate a substantial loss of coherence or disruption of the shaped-charge jet.

Overall, the 100 mm configuration produced complete perforation with a continuous penetration channel. The main observed features were the relatively wide entrance region, slight jet deviation and local deformation around the entrance hole. Despite these effects, the channel remained coherent along the full wall thickness.

(a) (b) (c)

Figure 6. Sectioned sample and entrance hole produced by the 3D-printed copper-filled liner at 100 mm stand-off distance: (a) left section of the penetration channel; (b) right section of the penetration channel; (c) front view of the entrance hole.

4.2 Result at 150 mm stand-off distance

Figures 7(a) and 7(b) show the left and right sections of the penetration channel produced in the steel cylinder segment by the charge equipped with a 3D-printed copper-filled liner at a stand-off distance of 150 mm. Figure 7(c) shows the corresponding front view of the entrance hole. As in the previous case, both parts of the sectioned penetration channel are presented in order to evaluate the internal morphology of the perforation and the deformation of the surrounding material.

The entrance region is visibly wider and more deformed than the exit opening. Pronounced uplift of the surrounding material can be observed around the entrance hole, indicating a strong interaction between the jet and the target surface during the initial phase of penetration. Compared with the 100 mm configuration, the entrance area appears less regular and shows a more pronounced lateral deformation of the target material.

The penetration channel remains continuous through the wall thickness, and complete perforation of the steel wall was achieved. However, the internal morphology of the channel is less regular than in the 100 mm sample. The channel wall contains local irregularities and cavity-like areas, especially in the central part of the perforation path. These features may indicate a reduction in jet coherence or a less stable interaction between the jet and the target material at the increased stand-off distance. Unlike the lower stand-off distance samples, pronounced scaly tearing or cracking of the surrounding material is not clearly visible.

The channel also shows noticeable variations in diameter along its length. The exit hole is very narrow and comparatively clean, but the internal channel does not retain a uniform geometry. A slight deviation of the penetration path from the charge axis is visible, although it is less pronounced than in the 100 mm sample. This suggests that the shaped-charge jet was still capable of fully perforating the target, but its effect was less regular and possibly less concentrated.

Overall, the 150 mm configuration also produced complete perforation. However, compared with the 100 mm sample, the penetration channel showed more pronounced diameter variations, local cavity-like features and less regular internal morphology. These features indicate a visible reduction in penetration quality at the largest tested stand-off distance.

(a) (b) (c)

Figure 7. Sectioned sample and entrance hole produced by the 3D-printed copper-filled liner at 150 mm stand-off distance: (a) left section of the penetration channel; (b) right section of the penetration channel; (c) front view of the entrance hole.

4.3 Combined comparison of stand-off distances

Because precise dimensional measurements were limited, the results were summarized using the qualitative visual criteria defined in Section 3.3. The comparison focuses on the morphology of the penetration channel rather than on exact numerical penetration parameters (Table 2). This approach makes it possible to compare the newly tested stand-off distances of 100 and 150 mm with the previous results obtained at 0, 15, 30 and 60 mm. Particular attention was paid to the entrance and exit hole appearance, channel wall morphology, tapering, jet alignment and the quality of the exit-side edge.

Table 2. Qualitative comparison of penetration morphology at different stand-off distances

Stand-off distance	Entrance hole	Exit hole	Channel wall morphology	Channel tapering	Jet alignment	Exit-side edge quality
0 mm	Narrow and clean entrance hole without visible material uplift	Wide exit hole with pronounced material tearing	Initially relatively smooth channel wall, followed by pronounced scaly tearing towards the exit side; visible cracking around the perforation and rough cut edges	Channel progressively widens from the entrance towards the exit	Approximately symmetrical	Rough and torn exit-side edge with pronounced material pull-out around the exit
15 mm	Slight material uplift around the entrance; wider entrance opening compared with 0 mm	Exit hole approximately symmetrical with the entrance opening	Initially relatively smooth channel wall, followed by local scaly tearing towards the exit side; minor cracking around the perforation and slightly rough cut edges	Channel remains relatively uniform along most of its length	Slightly misaligned	Pronounced frayed edge around the exit
30 mm	Wider entrance hole with local material loss and slight material uplift	Exit hole generally symmetrical, with a larger diameter	No pronounced scaly tearing; no visible cracking in the surrounding material; slightly roughened cut edge	Entrance and exit regions are wider than the central section of the channel	Slight deviation visible from approximately the middle of the channel	Minor burr formation with limited material pull-out
60 mm	Clean, relatively wide entrance base with slight material uplift and no significant burr formation	Narrow and regular exit hole	Clean channel wall without visible scaly tearing; edges appear relatively smooth and regular	Hourglass-like channel shape, without pronounced diameter variations	Approximately symmetrical	Clean exit-side edge with minimal burr formation
100 mm	Very wide entrance hole with pronounced lateral material uplift	Very narrow exit hole	Rough channel wall, without visible scaly tearing or cracking in the surrounding material	Channel narrows towards the exit side, with minor local diameter variations	Evidently misaligned	Local deformation around the entrance region; exit-side edge remains comparatively limited
150 mm	Deformed and wide entrance region with pronounced uplift of the surrounding material	Very narrow exit hole	Irregular channel wall; local cavities or discontinuous-looking areas may indicate reduced jet coherence; no visible cracking or scaly tearing	Pronounced diameter variations, especially in the central part of the channel	Slightly misaligned	Mild deformation around the entrance region; exit hole appears relatively clean

Row colours indicate the qualitative suitability of the tested stand-off distances. The white row represents the 0 mm configuration, which served primarily as a reference case confirming the functionality of the charge rather than as a true stand-off arrangement. The yellow row indicates an effective but less favourable configuration, where penetration was achieved but the effect appeared excessive for such a short stand-off distance. The light green rows represent a favourable operating range, in which the liner produced complete penetration with acceptable channel morphology. The dark green row denotes the most favourable result observed in this study, characterized by a relatively clean and regular penetration channel. The orange row indicates a visible reduction in penetration quality, especially in terms of channel regularity and diameter variation.
The comparison shows that complete perforation was achieved at all evaluated stand-off distances. Therefore, penetration alone is not sufficient to distinguish the influence of individual configurations. More relevant differences are visible in the morphology of the penetration channel, the deformation around the entrance and exit regions, and the regularity of the internal channel surface. The 30, 60, and 100 mm configurations represent the most practically meaningful range, with the 60 mm configuration showing the most favourable overall morphology. In contrast, the 150 mm configuration still produced complete perforation, but the irregular channel wall, pronounced diameter variations, and local cavity-like features suggest reduced jet coherence and a decrease in the quality of the penetration effect.

5. Discussion

The results confirm that copper-filled filaments processed by material extrusion can produce a functional shaped-charge effect. Although the tested liner was manufactured from a copper-filled polymer filament rather than from solid copper, it was capable of forming an accelerated jet or jet-like penetrator sufficient to perforate the steel target. This confirms the functional potential of additively manufactured shaped charge liners for experimental and specialized engineering applications.
The influence of stand-off distance was reflected primarily in the morphology of the penetration channels. All evaluated charges achieved complete perforation of the steel wall; therefore, complete penetration alone is not a sufficient criterion for assessing the effect of stand-off distance. More relevant differences were observed in the shape of the entrance and exit holes, the regularity of the penetration channel, the degree of material tearing, the presence of local cavity-like features, and the apparent alignment of the jet.
The results indicate that increasing the stand-off distance does not improve the effect indefinitely. Instead, the liner appears to have an effective operating range in which the jet remains sufficiently concentrated and produces a more regular penetration channel. The 0 mm configuration served primarily as a reference case confirming the functionality of the liner-equipped charge. However, it cannot be considered a true shaped-charge stand-off configuration, because the formation and stabilization of the jet depend on the distance between the liner and the target.
At 15 mm, the charge remained effective, but the observed morphology indicates excessive local interaction with the target. The most favourable behaviour was observed at 60 mm, where the penetration channel was comparatively clean and regular, with limited burr formation. The 30 and 100 mm configurations also remained within a practically meaningful range, although the 100 mm sample showed more pronounced entrance deformation and visible jet misalignment. In contrast, the 150 mm configuration still produced complete perforation, but the irregular channel wall, pronounced diameter variations, and local cavity-like features indicate a visible reduction in penetration quality and probable decrease in jet coherence.
From a practical perspective, these results are relevant mainly for applications where the objective is not maximum penetration depth, but controlled perforation or opening of a target. This is particularly important in EOD and C-IED tasks, where shaped charges may be used to perforate or disrupt ammunition casings in a controlled manner. In such cases, an extended stand-off distance may be useful if it allows the charge to remain effective while increasing the separation between the charge and the explosive content of the target munition. The results suggest that this may be feasible within a certain range, but that excessive stand-off distance can reduce the regularity and quality of the penetration effect.
Future work should therefore focus on defining the effective stand-off range more precisely and on determining whether similar results can be achieved with lower explosive masses. Reducing the explosive mass while maintaining sufficient perforation capability would improve controllability and could increase the practical relevance of additively manufactured shaped charge systems for specialized engineering, EOD, and C-IED applications.

Limitations

The main limitation of this study is the restricted number of specimens, with only one sample tested for each stand-off distance. This prevents statistical evaluation and means that the observed trends should be interpreted as indicative rather than conclusive. In addition, all charges were initiated within a single firing sequence. Although this ensured broadly consistent test conditions, possible mutual interaction effects between individual charges cannot be fully excluded.
The evaluation was primarily qualitative, as only limited dimensional measurements of the penetration channels were available. The conclusions are therefore based mainly on visual comparison of sectioned samples and photographic documentation. Moreover, the target was not sufficiently thick to determine the maximum penetration capability of the charges, so the results should be interpreted as a comparison of penetration morphology rather than ultimate penetration performance.
Further limitations are related to the liner material and explosive filling. The CopperFill liner is a copper-filled polymer composite and cannot be considered equivalent to a conventionally manufactured solid copper liner. Its material structure, density and collapse behaviour differ from those of metallic copper, and the material extrusion process may introduce layer-

related anisotropy or internal defects. Finally, the plastic explosive was manually pressed into the charge body, so perfect density uniformity cannot be guaranteed. Future experiments should therefore include repeated samples, more precise dimensional measurements, thicker targets and a more controlled filling procedure.

Conclusions

The presented follow-up experiment confirmed that 3D-printed copper-filled liners manufactured by material extrusion are capable of producing a functional shaped-charge effect. All evaluated configurations achieved complete perforation of the steel cylinder wall, including the newly tested stand-off distances of 100 and 150 mm. This confirms that the tested liner configuration remains effective beyond the originally evaluated range of 0–60 mm.

However, the results also show that complete perforation alone is not sufficient for assessing the influence of stand-off distance. More meaningful differences were observed in the morphology of the penetration channel, the regularity of the entrance and exit holes, the degree of material deformation, and the apparent alignment of the jet. The 0 mm configuration served primarily as a reference case, while the 15 mm configuration remained effective but showed signs of excessive local interaction with the target.

The most favourable result was observed at 60 mm stand-off distance. This configuration produced the cleanest and most regular penetration morphology, with limited burr formation and a coherent channel shape. The 30 and 100 mm configurations also remained within a practically meaningful operating range. In contrast, the 150 mm configuration still achieved complete perforation, but the irregular channel wall, pronounced diameter variations, and local cavity-like features suggest a visible reduction in jet coherence and penetration quality.

From a practical perspective, the results indicate that additively manufactured copper-filled liners may be relevant for specialized engineering, EOD, and C-IED applications where the objective is controlled perforation or opening of a target rather than maximum penetration depth. The possibility of increasing the stand-off distance while retaining sufficient perforation capability may be useful for reducing the risk of unwanted detonation transfer when working with hazardous ammunition.

Further research should focus on repeated testing, more precise dimensional measurements, thicker target configurations, and a more controlled explosive filling procedure. Future experiments should also examine whether similar perforation effects can be achieved with reduced explosive mass, which would improve controllability and practical applicability of 3D-printed shaped charge systems.

Acknowledgements. This work was conducted within the framework of the project "Conduct of land operations (DZRO-FVL22-LANDOPS)" and "Use of autonomous means in the minelaying process (SV24-FVL-K108-BIL)".

References

1. **Listek V**. Australian Military 3D Prints Over a Dozen Armoured Vehicle Parts in the Field, 3DPrint.com | Additive Manufacturing Business. Accessed: Apr. 30, 2026, Available at: https://3dprint.com/286608/australian-military-3d-prints-over-a-dozen-armoured-vehicle-parts-in-the-field/
2. **Vítek M., Jelínek J., Vítek R.** Impact of additive manufacturing in military industry, 2024, METAL Conference Proceedings.
3. **Liu J., Yan C.** 3D Printing of Scaffolds for Tissue Engineering, 2018, 3D Printing.
4. **Švehlík M., Sedláček M., Hasilová K., Drábek J., Šlouf V**. Applications in Engineer and Artillery Support: Mathematical Modeling of Symphatetic Detonation, 2024, Challenges to National Defence in Contemporary Geopolitical Situation.
5. **Bilina M., Vítek M., Dražan T., Žižka P.** Effectiveness of 3D Printed Shaped Charge Liners in Demolitions, 2025, International Conference on Military Technologies (ICMT).
6. **Carlucci D. E., Jacobson S. S.** Ballistics: Theory and Design of Guns and Ammunition, 2018, Third edition. Boca Raton: CRS Press.
7. **Hrnčiar M., Kompan J., Nohel J.** The future of the battlefield: Technology-driven predictions in the land domain, Revista Científica General José María Córdova, 2025, vol. 23(49), p.277–296.
8. **Voort G. F. V.** Metallography, Principles and Practice, 1999, Materials Park, Ohio: ASM International.
9. **ColorFabb PLA specialFill - Public sharing,** ColorFabb, 2026, Available at: https://downloads.colorfabb.com/index.php/s/rtfDDRCa723Xdor.